New Dinuclear Nickel(II) Complexes: Synthesis, Structure, Electrochemical, and Magnetic Properties

Dmitry Yakhvarov,*[†,§] Ekaterina Trofimova,[†] Oleg Sinyashin,[†] Olga Kataeva,[†,§] Yulia Budnikova,[†] Peter Lönnecke,[‡] Evamarie Hey-Hawkins,*[‡] Andreas Petr,*[§] Yulia Krupskaya,[§] Vladislav Kataev,[§] Rüdiger Klingeler,[§] and Bernd Büchner[§]

[†]A.E. Arbuzov Institute of Organic and Physical Chemistry of the Russian Academy of Sciences, Arbuzov Street 8, Kazan 420088, Russian Federation

[‡]Institute of Inorganic Chemistry, Universität Leipzig, Johannisallee 29, 04103 Leipzig, Germany

[§]IFW Dresden, POB 270116, D-01171, Dresden, Germany

S *Supporting Information*

ABSTRACT: The reaction of $[NiBr_2(bpy)_2]$ (bpy = 2,2′-bipyridine) with organic phosphinic acids $ArP(O)(OH)H$ [Ar = Ph, 2,4,6-trimethylphenyl (Mes), 9-anthryl (Ant)] leads to the formation of binuclear nickel(II) complexes with bridging $ArP(H)O_2^-$ ligands. Crystal structures of the binuclear complexes $[Ni_2(\mu\text{-}O_2P\text{-}(H)Ar)_2(bpy)_4]Br_2$ (Ar = Ph, Mes, Ant) have been determined. In each structure, the metal ions have distorted octahedral coordination and are doubly bridged by two arylphosphinato ligands. Magnetic susceptibility measurements have shown that these complexes display strong antiferromagnetic coupling between the two nickel atoms at low temperatures, apparently similar to binuclear nickel(II) complexes with bridging carboxylato ligands. Cyclic voltammetry and in situ EPR spectroelectrochemistry show that these complexes can be electrochemically reduced and oxidized with the formation of Ni(I),Ni(0)/Ni(III) derivatives.
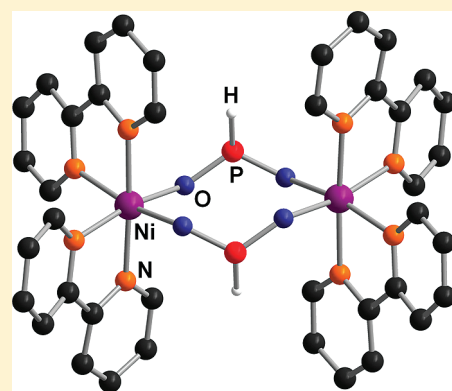
INTRODUCTION

Since the pioneering work of Tomic[1] in 1965 and Hoskins and Robson[2] in the 1990s on a new class of solid polymeric materials, currently known as metal—organic frameworks (MOF) or coordination polymers, mono- and polynuclear coordination compounds in which metal centers are connected by organic linkers have become important in various research areas.[3] Currently, these compounds are of great interest due to their potential practical applications.[4] Binuclear organometallic complexes of nickel(II), zinc(II), cobalt(II), and manganese(II) were found to be important intermediates in biological systems which catalyze the hydrolysis of a range of peptide and phosphate ester bonds via the formation of O—P—O bridged organometallic derivatives.[5] These species play a central role in biological processes of oxidative phosphorylation,[6] oxidative decarboxylation,[7] and energy transduction.[8] From the viewpoint of materials chemistry, organic—inorganic hybrids are an important class of compounds in advanced materials design.[9] Some nickel diphosphonates[10] and nickel pyrophosphates[11] showed antiferromagnetic properties and slow relaxation behavior. As a variant of polymetallic nickel complexes with O—P—O bridges, some nickel phosphonate—carboxylate cages bearing 12 nickel centers were synthesized.[12] Interestingly, a number of pentacoordinate nickel(II) complexes doubly bridged by phosphate ester or phosphinate ligands were synthesized and investigated.[13] However, currently, no examples of dinuclear nickel phosphinate complexes

(i.e., formed by bridging $RP(H)O_2$ ligands containing a PH group) are known. Only one dinuclear complex, formed by aluminum cations and bridging $RP(H)O_2$ ligands, is currently known.[14] The presence of a P—H bond in the bridging ligand creates the possibility of direct functionalization of the obtained polymer at phosphorus and thus allows the properties of the material to be modified.

Here, we describe the synthesis, structure, magnetic, and electrochemical properties of new dinuclear nickel complexes with bridging $ArP(H)O_2$ ligands [Ar = Ph, 2,4,6-trimethylphenyl (Mes), 9-anthryl (Ant)] bearing a PH group.

EXPERIMENTAL SECTION

All reactions and manipulations were carried out under dry, pure nitrogen in a standard Schlenk apparatus. THF and *n*-hexane were distilled from sodium/benzophenone and stored under nitrogen before use. CCl_4 and ethanol were purified by distillation. DMF was dried by stirring with calcium hydride (10 g/L) for 2 h and then distilled at a low pressure. After purification, all solvents were stored under an atmosphere of dry nitrogen. 2,2′-Bipyridine (99%, Alfa Aesar), $NiBr_2 \cdot 3H_2O$ (Fluka), $(NBu_4)BF_4$ (Acros Organics), and $PhPCl_2$ (Acros Organics) are commercially available and were used without additional purification. The electrolyte $(NBu_4)BF_4$ was dried by melting in a vacuum before use.

Table 1. Crystallographic Data for Complexes 3a−c

complex	3a	3b·2DMF	3c
empirical formula	$C_{58}H_{56}Br_2N_8Ni_2O_4P_2$	$C_{74}H_{65\cdot84}Br_{2\cdot17}N_{10}Ni_2O_6P_2$	$C_{52}H_{44}Br_2N_8Ni_2O_4P_2$
fw	1268.29	1543.57	1184.13
temp	198(2) K	130(2) K	130(2) K
wavelength	0.71073 Å	0.71073 Å	0.71073 Å
cryst syst	monoclinic	monoclinic	triclinic
space group	$P2_1/c$	$P2_1/c$	$P\bar{1}$
a	11.908(1) Å	13.5067(5) Å	8.5586(2) Å
b	15.051(1) Å	21.2589(6) Å	11.2437(3) Å
c	16.906(1) Å	12.1901(4) Å	13.7659(4) Å
α	90°	90°	67.180(3)°
β	109.31(1)°	103.476(4)°	86.841(2)°
γ	90°	90°	87.092(2)°
V	2859.6(3) Å^3	3403.9(2) Å^3	1218.53(6) Å^3
Z	2	2	1
ρ (calculated)	1.473 Mg/m^3	1.506 Mg/m^3	1.614 Mg/m^3
abs coeff	2.165 mm^{-1}	1.933 mm^{-1}	2.534 mm^{-1}
F(000)	1296	1579	600
cryst size	0.70 × 0.67 × 0.38 mm	0.35 × 0.14 × 0.07 mm	0.4 × 0.2 × 0.04 mm
θ range for data collection	3.26 to 25°	3.10 to 30.51°	2.93 to 30.51°
index ranges	$-13 \leq h \leq 14$, $-17 \leq k \leq 17$, $-19 \leq l \leq 20$	$-19 \leq h \leq 18$, $-30 \leq k \leq 30$, $-14 \leq l \leq 17$	$-12 \leq h \leq 12$, $-16 \leq k \leq 16$, $-19 \leq l \leq 19$
reflns collected	38540	39248	27084
independent reflns	4915 [R(int) = 0.0378]	10353 [R(int) = 0.0382]	7437 [R(int) = 0.0345]
completeness to θ	97.8% (25°)	99.8% (30.51°)	99.9% (30.51°)
abs correction	semiempirical from equivalents	semiempirical from equivalents	semiempirical from equivalents
max./min transmission	0.4934/0.3126	1/0.88668	1/0.6132
refinement method	full-matrix least-squares on F^2	full-matrix least-squares on F^2	full-matrix least-squares on F^2
data/restraints/params	4915/0/349	10353/51/492	7437/0/403
goodness-of-fit on F^2	1.076	0.851	0.951
final R indices [I > 2σ(I)]	R1 = 0.0272, wR2 = 0.0598	R1 = 0.0305, wR2 = 0.0618	R1 = 0.0300, wR2 = 0.0696
R indices (all data)	R1 = 0.0427, wR2 = 0.0657	R1 = 0.0601, wR2 = 0.0646	R1 = 0.0468, wR2 = 0.0724
largest diff. peak and hole	0.518 and -0.364 e·Å^{-3}	0.619 and -0.593 e·Å^{-3}	1.335 and -0.495 e·Å^{-3}

Cyclic voltammograms were recorded at a glassy carbon (working surface 3.14 mm^2) in a thermostatically controlled (20 °C) three-electrode electrochemical cell under N_2 in the presence of $(NBu_4)BF_4$ (0.1 M) with a PI-50-1 potentiostat/galvanostat (USSR). The substrate concentration was 5×10^{-3} M. An Ag/AgNO$_3$ (0.01 mol·L^{-1} solution in CH$_3$CN) was used as a reference electrode and a platinum wire as an auxiliary electrode. Curves were recorded at a constant potential scan rate of 50 mV s^{-1}.

The NMR spectra were recorded on a Bruker MSL-400 (^{1}H 400 MHz, ^{31}P 161.9 MHz). SiMe$_4$ was used as an internal reference for ^{1}H NMR chemical shifts and 85% H$_3$PO$_4$ as an external reference for ^{31}P. IR spectra were recorded on a Bruker Vector-22 in the range 4000−400 cm^{-1} at a resolution of 4 cm^{-1}. Elemental analysis was performed on a EuroVector CHNS-O Elemental Analyzer EA3000. The nickel and phosphorus contents of the obtained compounds were determined by inductively coupled plasma mass spectrometry (ICP-MS) on a Perkin-Elmer Elan DRC II mass spectrometer (USA) and atomic absorption spectroscopy (AAS) on a Carl Zeiss AAS1 spectrometer. Static magnetic susceptibility was measured with a superconducting quantum interference device vibrating sample magnetometer (SQUID-VSM) from Quantum Design. The EPR measurements were performed with an X-Band (10 GHz) Bruker EMX spectrometer.

X-Ray Structure Determination. Crystallographic data for compounds **3a−c** are given in Table 1. The experimental details are provided in the Supporting Information.

Synthesis of Phosphinic Acids. *MesP(H)(O)OH (1a)*. A total of 8.21 g (37 mmol) of MesPCl$_2$, obtained by using a described procedure,[15] was slowly added to 13.3 mL (0.74 mol, 13.3 g) of distilled water cooled to +5 °C with vigorous stirring. After 15 min of stirring, a large amount of white precipitate was formed. After 4 h of stirring at room temperature, the solid was filtered off and dried in a vacuum (10^{-6} bar). Yield: 80.8% (5.5 g).

^{1}H NMR (C$_6$D$_6$): δ 1.94 (s, 3H, p-CH$_3$), 2.51 (s, 6H, o-CH$_3$), 6.51 (d, $^4J_{PH}$ = 4.4 Hz, 2H, m-H), 8.06 (d, $^1J_{PH}$ = 557 Hz, 1H, P−H), 11.52 (br, 1H, P−OH).

^{31}P NMR (C$_6$D$_6$): δ 23.6 ($^1J_{PH}$ = 557 Hz).

Anal. Calcd for C$_9$H$_{13}$O$_2$P (184.17): C, 58.69; H, 7.11; P, 16.82. Found: C, 59.05; H, 7.26; P, 16.94.

IR (KBr, cm^{-1}): 2974 (m, C−H$_{Mes}$), 2922 (m, C−H$_{Mes}$), 2854 (m, C−H$_{Mes}$), 2600 (br, s, P−OH), 2409 (m, P−H), 2272 (s, C−H$_{Mes}$), 2163 (s, C−H$_{Mes}$), 1656 (s, C=C$_{Mes}$), 1453 (m), 1415 (m), 1200 (s, P=O), 630 (s, C−H$_{Mes}$), 558 (s, C−H$_{Mes}$).

AntP(H)(O)OH (1b). A total of 6.4 mL (356 mmol) of freshly distilled and degassed water was added to a solution of 1.45 g (5.2 mmol) of AntPCl$_2$[16] in 30 mL of dichloromethane. After 3 h of stirring, the formed light yellow precipitate was filtered off and washed with two portions of cold dichloromethane (2 × 15 mL). After drying the formed precipitate in a vacuum, 0.75 g (63%) of **1b** was obtained. Compound **1b** is insoluble in dichloromethane, benzene, acetone, and water.
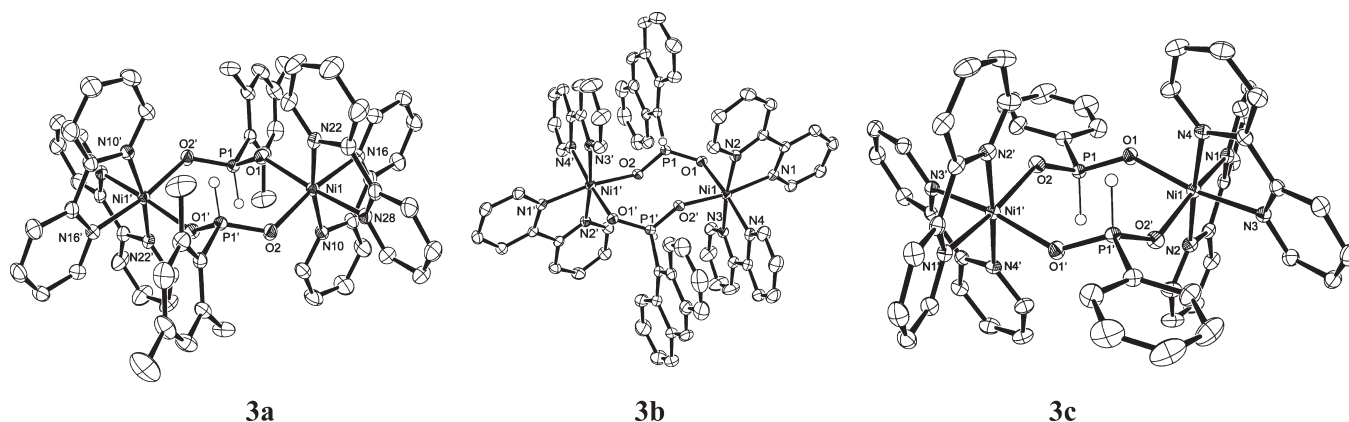
Figure 1. ORTEP drawings of the complex cations in **3a**−**c** with 50% probability displacement ellipsoids of non-H atoms.

^{1}H NMR (DMSO-d6): δ 3.83 (s, 1H, OH), 7.59 (t, $^1J_{HH}$ = 7.6 Hz, 2H, 3,6-H), 7.67 (t, $^1J_{HH}$ = 7.6 Hz, 2H, 2,7-H), 7.90 (s, 1H, 10-H), 8.19 (d, $^1J_{HH}$ = 7.6 Hz, 2H, 4,5-H), 8.60 (d, $^1J_{PH}$ = 560 Hz, 1H, P−H), 9.01 (d, $^1J_{HH}$ = 7.6 Hz, 2H, 1,8-H).

^{31}P NMR (DMSO-d6): δ 13.8 ($^1J_{PH}$ = 560 Hz).

Anal. Calcd for $C_{14}H_{11}O_2P$ (242.21): C, 69.42; H, 4.58; P, 12.79. Found: C, 69.05; H, 4.96; P, 12.64.

PhP(H)(O)OH (**1c**). Phenylphosphinic acid has been prepared according to a modified literature procedure.[17] A total of 26.8 g (150 mmol) of PhPCl$_2$ was slowly added with vigorous stirring to 80.0 mL of distilled and degassed water cooled to +5 °C. After 5 min a large amount of white precipitate formed. Stirring was continued for 4 h at room temperature. Then the solid was isolated by filtration, washed with water (2 × 100 mL) and diethyl ether (2 × 50 mL) and dried in vacuum (10^{-6} bar). Yield: 54.9% (11.7 g). ^{1}H NMR (C$_6$D$_6$): δ 6.93−7.04 (m, 3H, m-H, p-H), 7.47 (d, $^1J_{PH}$ = 567 Hz, 1H, P−H), 7.63−7.69 (m, 2H, o-H), 12.86 (br, 1H, P−OH). ^{31}P NMR (C$_6$D$_6$): δ 20.5 ($^1J_{PH}$ = 567 Hz).[18] Anal. Calcd for $C_6H_7O_2P$ (142.09): C, 50.72; H, 4.97; P, 21.80. Found: C, 50.28; H, 4.90; P, 21.48. IR (KBr, cm^{-1}): 2925 (w, C−H), 2848 (w, C−H), 2587 (br, s, P−OH), 2407 (m, P−H), 2165 (m, P(O)H), 1676 (w, C=C), 1439 (s, P−C$_6$H$_5$), 1198 (s, P=O), 988 (w), 751 (w, C−H), 693 (w, P−C), 534 (w, C−H).

Synthesis of the Complexes. *[NiBr$_2$(bpy)$_2$]* (**2**). [NiBr$_2$(bpy)$_2$] was prepared according to a modified procedure.[19] Solid NiBr$_2$·3H$_2$O (1.50 g, 5.5 mmol) was added to an ethanolic solution (90 mL) containing 1.72 g (11.0 mmol) of 2,2′-bipyridine. The solution was stirred for 3 h, and then the solvent was evaporated and the residue washed with diethyl ether (3 mL) and dried in a vacuum at 30 °C for 5 h. The yield of **2** was 2.45 g (84%).

IR (KBr, cm^{-1}): 1601 (s, C=N), 1573 (s, C=C), 1564 (m), 1493 (m), 1473 (m), 1441 (s), 1024 (m), 770 (s, C−H$_{bpy}$), 735 (s, C−H$_{bpy}$).

[Ni$_2$(μ-O$_2$P(H)Mes)$_2$(bpy)$_4$]Br$_2$ (**3a**). A total of 30 mL of a DMF solution containing 1.47 g (8.0 mmol) of MesP(H)(O)OH was added to a solution containing 4.25 g (8.0 mmol) of [NiBr$_2$(bpy)$_2$] in 20 mL of DMF under continuous stirring. The color of the solution changed from light green to blue-green. The addition of diethyl ether resulted in the formation of dark-green crystals of **3a** suitable for X-ray crystal structure analysis. Yield: 3.60 g (71%).

Anal. Calcd for $C_{58}H_{56}Br_2N_8Ni_2O_4P_2$ (1268.26): C, 54.93; H, 4.45; Br, 12.60; N, 8.84; Ni, 9.26; P, 4.88. Found: C, 55.09; H, 4.64; Br, 12.98; N, 8.98; Ni, 9.17; P, 4.42.

IR (KBr, cm^{-1}): 3096 (w, C−H$_{Mes}$), 3042 (w, C−H$_{Mes}$), 3018 (w, C−H$_{Mes}$), 2975 (w, C−H$_{Mes}$), 2393 (w, P−H), 1657 (s, C=C$_{Mes}$), 1597 (s, C=N$_{bpy}$), 1562 (m, C=C$_{bpy}$), 1490 (w), 1468 (m), 1439 (s), 1310 (m, PO$_2$), 1016 (m), 904 (w), 776 (s, C−H$_{bpy}$), 733 (m, C−H$_{bpy}$).

[Ni$_2$(μ-O$_2$P(H)Ant)$_2$(bpy)$_4$]Br$_2$ (**3b**). A total of 7 mL of a DMF solution containing 0.19 g (0.8 mmol) of AntP(H)(O)OH was slowly added to a solution containing 0.42 g (0.8 mmol) of [NiBr$_2$(bpy)$_2$] in 8 mL

of DMF with continuous stirring. After 8 days at room temperature, blue crystals of **3b**·2DMF had formed in solution. Yield: 0.28 g (46%).

Anal. Calcd for $C_{74}H_{66}Br_2N_{10}Ni_2O_6P_2$ (1530.52): C, 58.07; H, 4.35; Br, 10.44; N, 9.15; Ni, 7.67; P, 4.05. Found: C, 57.69; H, 4.48; Br, 10.35; N, 9.21; Ni, 7.38; P, 4.02.

IR (KBr, cm^{-1}): 3013 (m), 2410 (m, P−H), 1664 (s, C=N), 1598 (s, C=C), 1443 (s), 1453 (m), 1171 (s, PO$_2$), 1046 (s, P−C), 1022 (m), 765 (s), 459 (s, Ni−O).

Crystals for X-ray analysis were obtained from a different batch of AntP(H)(O)OH that contained 10-Br-substituted Ant as an impurity (**3b**·2DMF, $C_{74}H_{65.84}Br_{2.17}N_{10}Ni_2O_6P_2$, 1543.57) and showed the presence of anthracene/bromoanthracene disordered in a ratio 0.92/0.08.

*[Ni$_2$(μ-O$_2$P(H)Ph)$_2$(bpy)$_4$]Br$_2$* (**3c**). A total of 2 mL of a DMF solution containing 0.12 g (0.85 mmol) of PhP(H)(O)OH was slowly added to a solution containing 0.45 g (0.85 mmol) of [NiBr$_2$(bpy)$_2$] in 4.5 mL of DMF under continuous stirring. After one day at room temperature, blue-green crystals of **3c** had formed. Yield: 2.18 g (71%).

Anal. Calcd for $C_{52}H_{44}Br_2N_8Ni_2O_4P_2$ (1184.10): C, 52.75; H, 3.75; Br, 13.50; N, 9.46; Ni, 9.91; P, 5.23. Found: C, 52.01; H, 3.94; Br, 13.98; N, 9.98; Ni, 9.36; P, 4.88.

IR (KBr, cm^{-1}): 3197 (w), 3099 (w), 3015 (w), 2975 (w), 2323 (s, P−H), 1596 (s, C=N), 1572 (m, bpy), 1437 s, P−C$_6$H$_5$), 1305 (s), 1201 (s), 1056 (s, PO$_2$), 773 (s, P−C), 564 (m, Ni−O).

■ RESULTS AND DISCUSSION

Syntheses. Complexes **3a**−**c** were prepared from aromatic phosphinic acids MesP(H)(O)OH (Mes = 2,4,6-trimethylphenyl, **1a**), AntP(H)(O)OH (Ant = 9-anthryl, **1b**), and PhP(H)-(O)OH and [NiBr$_2$(bpy)$_2$] (**2**, bpy = 2,2′-bipyridine) in dimethylformamide (DMF) solution (eq 1).

$$2[NiBr_2(bpy)_2] + 2ArP(H)(O)OH \xrightarrow{-2HBr} \textbf{3a-c} \quad (1)$$

Ar = Mes (a), Ant (b), Ph (c)
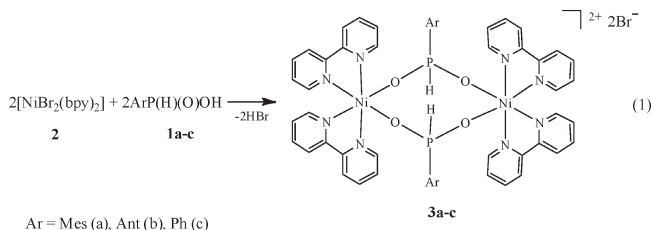
These complexes are the first examples of dinuclear nickel complexes with bridging ArP(H)O$_2$ ligands, whereas the first examples of related dinuclear organoaluminum complexes were published in 2002.[14] The major interest in systems containing PH groups lies in the possibility of direct functionalization of their corresponding coordination polymers by modification of

Table 2. Selected Bond Lengths (Å) and Angles (deg) for Complexes 3a–c

3a	3b	3c
Ni(1)–O(2) 2.039(2)	Ni(1)–O(2) 2.057(1)	Ni(1)–O(2) 2.059(1)
Ni(1)–O(1) 2.049(2)	Ni(1)–O(1) 2.068(1)	Ni(1)–O(1) 2.050(1)
P(1)–O(2) 1.505(2)	P(1)–O(2) 1.506(1)	P(1)–O(2) 1.503(1)
P(1)–O(1) 1.504(2)	P(1)–O(1) 1.504(1)	P(1)–O(1) 1.499(1)
P(1)–C(1) 1.809(2)	P(1)–C(1) 1.819(2)	P(1)–C(1) 1.799(2)
O(1)–Ni(1)–O(2) 91.36(7)	O(1)–Ni(1)–O(2) 90.51(4)	O(1)–Ni(1)–O(2) 95.25(5)
O(1)–P(1)–O(2) 116.4(1)	O(1)–P(1)–O(2) 117.12(7)	O(1)–P(1)–O(2) 117.97(8)
Ni(1)–O(1)–P(1) 135.4(1)	Ni(1)–O(1)–P(1) 120.85(7)	Ni(1)–O(1)–P(1) 136.60(8)
Ni(1)–O(2)–P(1) 125.7(1)	Ni(1)–O(2)–P(1) 132.38(7)	Ni(1)–O(2)–P(1) 135.93(8)
O(1)–Ni(1)–O(2)–P(1) −18.9(1)	O(1)–Ni(1)–O(2)–P(1) 84.5(1)	O(1)–Ni(1)–O(2)–P(1) 51.0(1)
Ni(1)–O(1)–P(1)–O(2) 134.1(1)	Ni(1)–O(1)–P(1)–O(2) 77.20(9)	Ni(1)–O(1)–P(1)–O(2) 92.8(1)
Ni(1)–O(2)–P(1)–O(1) −79.7(1)	Ni(1)–O(2)–P(1)–O(1) 142.95(8)	Ni(1)–O(2)–P(1)–O(1) 104.1(1)

the PH bond, which may lead to new types of catalysts and magnetoactive materials.[20]

Molecular Structures. According to single-crystal X-ray diffraction crystallographic data given in Table 1, nickel complexes **3a–c** form centrosymmetric dimers in which the two Ni atoms are bridged by two $O_2P(H)Ar^-$ ligands (Figure 1). The P–O–Ni-containing eight-membered heterocycles adopt a chair conformation in **3a** and **3b** and a long chair conformation in **3c**. The flattening of the heterocycle in **3c** results in larger endocyclic O–Ni–O bond angles of up to 95.2° as opposed to 91.4° in **3a** and 90.5° in **3b**. More pronounced changes are observed for the angles at oxygen (Ni–O–P): 135.9 and 136.6° in **3c**, 125.7 and 135.4° in **3a**, and 120.9 and 132.4° in **3b** (selected geometrical parameters are given in Table 2). Phosphorus coordination is very similar in all compounds. The nickel atoms have slightly distorted octahedral coordination with a *cis* arrangement of the oxygen atoms. A drastically different orientation of aromatic substituents at phosphorus is observed depending on their volume. The smallest Ph substituent in **3c** is nearly eclipsed with the phosphorus–oxygen bonds, while the bulky Mes and Ant substituents in **3a** and **3b** adopt an almost perpendicular orientation. The Ant substituents slightly deviate from ideal bisector orientation, so that a parallel arrangement of Ant and bpy ligands is realized to promote intramolecular $\pi-\pi$ interaction with an interplanar distance of 3.3 Å.

Magnetic Measurements. The static magnetic susceptibility χ of powder samples of **3a** and **3b** was measured in a magnetic field of 1 T at 2–300 K. The two samples show very similar behavior. The experimental data for **3a**, which are representative for both samples, are shown in Figure 2. Except for the low-temperature region, the data can be very well fitted with the Curie–Weiss law $\chi = \chi_0 + C/(T - \theta)$, were C is the Curie constant, θ is the Curie–Weiss temperature, and χ_0 is the temperature-independent contribution to the susceptibility. From C, one can calculate the effective magnetic moment $\mu_{eff} = g[(S_{eff} + 1)S]^{1/2}$, which amounts to 3.21 μ_B per Ni ion. This value corresponds to a spin of $S_{eff}^{Ni} = 1.14$ (assuming the g factor of 2.052 obtained from ESR measurements; see below). The obtained Curie–Weiss temperature of $\theta = 1.4$ K indicates a weak antiferromagnetic (AFM) interaction between two nickel ions within the molecule. A strong deviation of the experimental data from the Curie–Weiss law in the low-temperature regime ($T < 10$ K) is also suggestive of an AFM coupling of the nickel ions, which significantly decreases the susceptibility of the complex at low temperatures (Figure 2, upper inset). Finally, the AFM coupling
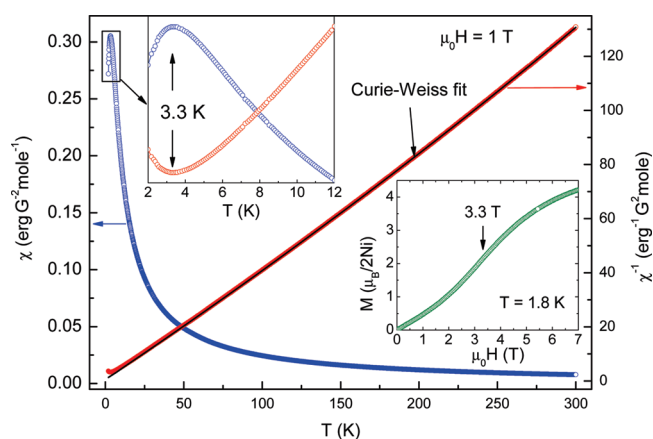
Figure 2. Temperature dependence of the magnetic susceptibility $\chi(T)$ and of the reciprocal susceptibility $\chi^{-1}(T)$ for **3a**. The black line represents the Curie–Weiss fit to the experimental data at $T > 100$ K. The upper inset shows an enlarged view of $\chi(T)$ and $\chi^{-1}(T)$ in the temperature range 2–12 K. The lower inset shows the magnetic field dependence of the static magnetization of **3a** at $T = 1.8$ K.

was confirmed by measurements of the magnetic field dependence of the static magnetization $M(H)$ at $T = 1.8$ K (Figure 2, lower inset). The observed S-shaped bending of the magnetization curve at about 3.3 T indicates breaking of the AFM coupling with increasing magnetic field. With a further increase of the field strength, the magnetization tends to saturate at a value of about 4.4 μ_B somewhat above 7 T. The saturation magnetization $M_S = gS^{tot}\mu_B \approx 4.4\ \mu_B$ corresponds to an effective total spin of the molecule of $S_{eff}^{tot} \approx 2$ and, thus, provides evidence for a parallel alignment of the spins of the nickel ions in the magnetic field.

Electrochemical and EPR Studies. The electrochemical properties of complexes **3a–c** were investigated by cyclic voltammetry (CV). All investigated complexes display the same electrochemical behavior with identical CV curves. Two reversible reduction peaks are present in the CV curve of dinuclear complex **3a** (Figure 3). The first reduction peak C_1 ($E_P^{red} = -1.70$ V vs Ag/Ag$^+$) corresponds to the reduction of nickel (Ni^{II}/Ni^0, eq 2) and the second peak C_2 ($E_P^{red} = -2.30$ V vs Ag/Ag$^+$) to reduction of the coordinated 2,2′-bipyridine ligand (eq 3).

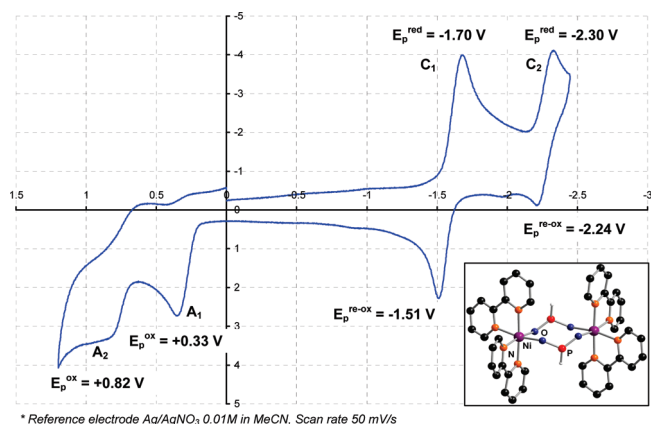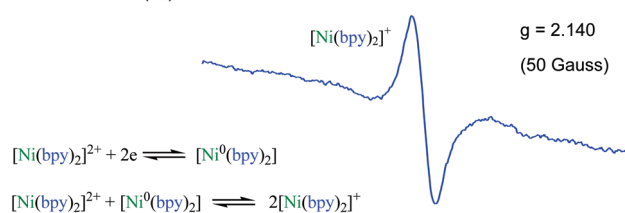$$[Ni(bpy)_2]^{2+} \rightleftharpoons [Ni^0(bpy)_2] \qquad (2)$$
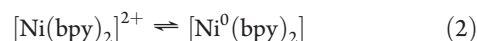
Figure 3. Cyclic voltammogram of **3a** in DMF (room temperature).

Electroreduction (**C₁**)

$$[Ni(bpy)_2]^{2+} + 2e \rightleftharpoons [Ni^0(bpy)_2]$$

$$[Ni(bpy)_2]^{2+} + [Ni^0(bpy)_2] \rightleftharpoons 2[Ni(bpy)_2]^+$$

Electroreduction (**C₂**)

$$[Ni^0(bpy)_2] + e \rightleftharpoons [Ni(bpy)_2]^{\cdot -}$$

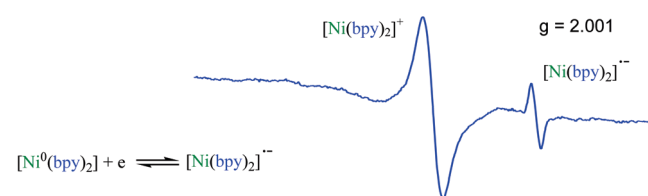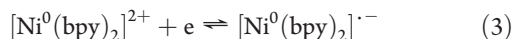**Figure 4.** EPR spectra of **3a** in solution (DMF) at room temperature after 2F (top curve) and after 4F (bottom curve).

$$[Ni^0(bpy)_2]^{2+} + e \rightleftharpoons [Ni^0(bpy)_2]^{\cdot -} \qquad (3)$$

Monitoring of the electrochemical process by in situ EPR spectroelectrochemistry allowed us to make some conclusions concerning the mechanism of reduction. The EPR powder spectrum of the complex displays one very broad signal ($g = 2.052$, broadness about 500 G) corresponding to paramagnetic nickel(II) with $S = 1$. However, no signals were observed in DMF solution at room temperature.

A new signal with $g = 2.140$ (broadness 50 G) appears when the cathodic potential is applied (Figure 4). This signal corresponds to the reduced form of the metal center with a d^9 electron configuration, i.e., nickel(I). Interestingly, after passing 2F, i.e., two e⁻ per molecule of dinuclear complex **3a**, only the signal corresponding to the reduced nickel(I) form is observed in the EPR spectra (Figure 4, top curve).

However, this signal disappears upon exhaustive electrolysis, resulting in the formation of the nickel(0) complex (after 4F), and a new anionic radical form of the complex containing a coordinated bpy radical anion ($g = 2.001$, Figure 4) is formed due to electroreduction at peak **C₂** ($E_p^{red} = -2.30$ V vs Ag/Ag⁺; Figure 4, bottom curve). Monitoring the electroreduction

Electroreduction

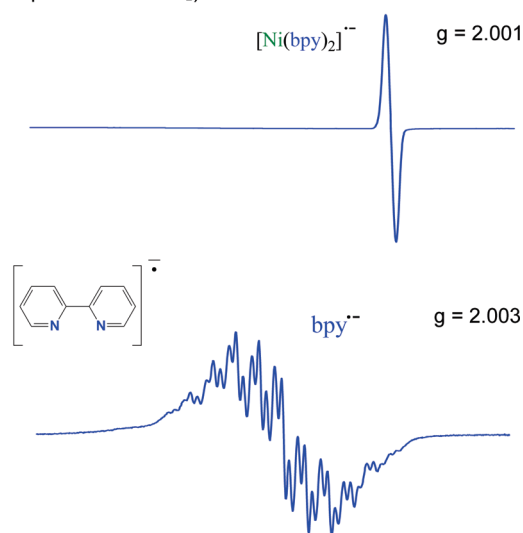(higher cathodic potentials than **C₂**)

Figure 5. EPR spectra of DMF solution containing **3a** at room temperature (exhaustive electroreduction).

process at high cathodic potentials (greater than -2.50 V vs Ag/Ag⁺) leads to the decomposition of complex **3a**, and the signal of the free bpy radical anion ($g = 2.003$) is observed in the EPR spectrum of the reaction mixture (Figure 5). This g factor is also observed for the free bpy radical anion in acetonitrile.[21] The well-resolved hyperfine structure of the signal is another reason to assign it to the uncoordinated bpy anion radical.

The electrochemical oxidation of complexes **3a–c** involves two quasi-reversible one-electron processes **A₁** ($E_p^{ox} = +0.33$ V vs Ag/Ag⁺) and **A₂** ($E_p^{ox} = +0.82$ V vs Ag/Ag⁺). The first oxidation peak **A₁** corresponds to oxidation of the bromide counterions of dicationic binuclear nickel complexes **3a–c**. The same oxidation peak is observed in the CV curve of a DMF solution containing n-Bu₄NBr (5×10^{-3} M) and supporting electrolyte n-Bu₄NBF₄ (0.1 M). The second oxidation peak **A₂** corresponds to the oxidation of nickel(II) to nickel(III). These electrochemical processes are quasi-reversible one-electron oxidation couples with the formation of Ni^II Ni^III and Ni^III Ni^III complexes, as has been shown for related dinuclear nickel complexes with bridging anionic carboxylato groups.[22,23]

■ CONCLUSIONS

New dimetallic nickel(II) complexes with bridging phosphinato ligands (O₂P(H)Ar⁻, Ar = Ph, 2,4,6-trimethylphenyl, 9-anthryl) display strong antiferromagnetic coupling between the two nickel atoms at low temperatures. Furthermore, the spin state of the nickel centers can be easily changed by electrochemical reduction/oxidation in solution, leading to new nickel complexes in different oxidation states, and this can be regarded as a new tool for tuning the magnetic properties of these dinuclear nickel complexes.

■ ASSOCIATED CONTENT

ⓢ Supporting Information. Additional X-ray structure determination information and crystallographic data (CIF format) are available free of charge via the Internet at http://pubs.acs.org.

■ AUTHOR INFORMATION

Corresponding Author

*Fax: +7-843-2732253 (D.Y.), +49-341-9739319 (E.H.-H.), +49-351-4659313 (A.P.). E-mail: yakhvar@iopc.ru (D.Y.), hey@uni-leipzig.de (E.H.-H.) a.petr@ifw-dresden.de (A.P.).

■ REFERENCES

(1) Tomic, E. A. *J. Appl. Polym. Sci.* **1965**, *9*, 3745–3752.

(2) Hoskins, B. F; Robson, R. *J. Am. Chem. Soc.* **1990**, *112*, 1546–1554.

(3) (a) James, S. L. *Chem. Soc. Rev.* **2003**, *32*, 276–288. (b) Ockwig, N. W.; Delgado-Friedrichs, O.; O'Keeffe, M.; Yaghi, O. M. *Acc. Chem. Res.* **2005**, *38*, 176–182.

(4) (a) Noro, S.; Kitagawa, S.; Kondo, M.; Seki, K. *Angew. Chem.* **2000**, *112*, 2161–2164; *Angew. Chem., Int. Ed. Engl.* **2000**, *39*, 2081–2084; (b) Kesanli, B.; Cui, Y.; Smith, M.; Bittner, E.; Bockrath, B.; Lin, W. *Angew. Chem.* **2005**, *117*, 74–77; *Angew. Chem., Int. Ed. Engl.* **2005**, *44*, 72–75; (c) Eddaoudi, M.; Kim, J.; Rosi, V.; Vodak, D.; Wachter, J.; O'Keeffe, M.; Yaghi, O. M. *Science* **2002**, *295*, 469–472; (d) Rosi, N. L.; Eckert, J.; Eddaoudi, M.; Vodak, D. T.; Kim, J.; O'Keeffe, M.; Yaghi, O. M. *Science* **2003**, *300*, 1127–1129; (e) Min, K. S.; Suh, M. P. *J. Am. Chem. Soc.* **2000**, *122*, 6834–6840; (f) Seo, J. S.; Wand, D.; Lee, H.; Jun, S. I.; Oh, J.; Jeon, Y.; Kim, K. *Nature* **2000**, *404*, 982–986; (g) Pan, L.; Liu, H.; Lei, X.; Huang, X.; Olson, D. H.; Turro, N. J.; Li, J. *Angew. Chem.* **2003**, *115*, 560–564; *Angew. Chem., Int. Ed. Engl.* **2003**, *42*, 542–546; (h) Kesanli, B.; Lin, W. *Coord. Chem. Rev.* **2003**, *246*, 305–326; (i) Wu, C. D.; Hu, A.; Zhang, L.; Lin, W. *J. Am. Chem. Soc.* **2005**, *127*, 8940–8941; (j) Wu, C. D.; Lin, W. *Angew. Chem.* **2007**, *119*, 1093–1096; *Angew. Chem., Int. Ed. Engl.* **2007**, *46*, 1075–1078; (k) Chen, B.; Liang, C.; Yang, J.; Contreras, D. S.; Clancy, Y. L.; Lobkovsky, E. B.; Yaghi, O. M.; Dai, S. *Angew. Chem.* **2006**, *118*, 1418–1421; *Angew. Chem., Int. Ed. Engl.* **2006**, *45*, 1390–1393. (l) Bordiga, S.; Lamberti, C.; Ricchiardi, G.; Regli, L.; Bonino, F.; Damin, A.; Lillerud, K. P.; Bjorgen, M.; Zecchina, A. *Chem. Commun.* **2004**, 2300–2301. (m) Ayyappan, P.; Evans, O. R.; Cui, Y.; Wheeler, K. A.; Lin., W. *Inorg. Chem.* **2002**, *41*, 4978–4980. (n) Kahn, O. *Acc. Chem. Res.* **2000**, *33*, 647–657.

(5) Wilcox, D. E. *Chem. Rev.* **1996**, *96*, 2435–2458.

(6) (a) Walker, J. E. *Angew. Chem.* **1998**, *110*, 2438–2450; *Angew. Chem., Int. Ed. Engl.* **1998**, 37, 2308–2319; (b) Boyer, P. D. *Angew. Chem.* **1998**, *110*, 2424–2436; *Angew. Chem., Int. Ed. Engl.* **1998**, 37, 2296–2307.

(7) Dorrestein, P. C.; Zhai, H.; Taylor, S. V.; McLafferty, F. W.; Begley, T. P. *Biochemistry* **2003**, *42*, 12430–12438.

(8) (a) Adams, R. L. P.; Knowler, J. T.; Leader, D. P. *The Biochemistry of Nucleic Acids*, 10th ed.; Chapman and Hall: New York, 1986. (b) Blackburn, G. M.; Gait, M. J. *Nucleic Acids in Chemistry and Biology*, 2nd ed.; Oxford University Press: New York, 1996. (c) Berg, J. M.; Tymoczko, J. L.; Stryer, L. *Biochemistry*, 5th ed.; W. H. Freeman and Company: New York, 2001.

(9) (a) Moulton, B.; Zaworotko, M. J. *Chem. Rev.* **2001**, *101*, 1629–1658. (b) Cantrill, S. J.; Chichak, K. S.; Peters, A. J.; Stoddart, J. F. *Acc. Chem. Res.* **2005**, *38*, 1–9. (c) Brage, D. *Chem. Commun.* **2003**, 2751–2754. (d) Seidel, S. R.; Stang, P. J. *Acc. Chem. Res.* **2002**, *35*, 972–983. (e) Fujita, M.; Umemoto, K.; Yoshizawa, M.; Fujita, N.; Kusukawa, T.; Biradha, K. *Chem. Commun.* **2001**, 509–518. (f) Férey, G.; Mellot-Draznieks, C.; Serre, C.; Millange, F. *Acc. Chem. Res.* **2005**, *38*, 217–225.

(10) Cao, D. K.; Yi-Zhi, L.; Zheng, L.-M. *Inorg. Chem.* **2007**, *46*, 7571–7578.

(11) Ikotun, O. F.; Armatus, N. G.; Julve, M.; Kruger, P. E.; Lloret, F.; Nieuwenhuyzen, M.; Doyle, R. P. *Inorg. Chem.* **2007**, *46*, 6668–6674.

(12) Breeze, B. A.; Shanmugam, M.; Tuna, F.; Winpenny, R. E. P. *Chem. Commun.* **2007**, 5185–5187.

(13) Santana, M. D.; Garcia, G.; Lozano, A. A.; Lopez, G.; Tudela, J.; Perez, J.; Garcia, L.; Lezama, L.; Rojo, T. *Chem.—Eur. J.* **2004**, *10*, 1738–1746.

(14) Azais, T.; Bonhomme-Coury, L.; Vaissermann, J.; Bertani, P.; Hirschinger, J.; Maquet, J.; Bonhomme, C. *Inorg. Chem.* **2002**, *41*, 981–988.

(15) (a) Freeman, S.; Harger, M. J. *J. Chem. Soc., Perkin Trans. 1* **1987**, 1399–1406. (b) Nief, F.; Mathey, F. *Tetrahedron* **1991**, *47*, 6673–6680.

(16) Yang, F.; Fanwick, P. E.; Kubiak, C. P. *Organometallics* **1999**, *18*, 4222–4225.

(17) Michaelis, A. *Justus Liebigs Ann. Chem.* **1876**, *181*, 265–363.

(18) Van Wazer, J. R.; Callis, C. F.; Shoolery, J. N.; Jones, R. C. *J. Am. Chem. Soc.* **1956**, *78*, 5715–5726.

(19) Troupel, M.; Rollin, Y.; Sock, O.; Meyer, G.; Perichon, J. *Nov. J. Chim.* **1986**, *10*, 593–599.

(20) Kristine, K.; Tanabe, M.; Cohen, S. *Angew. Chem., Int. Ed.* **2009**, *48*, 7424–7427.

(21) Kaim, W.; Ernst, S.; Kasak, V. *J. Am. Chem. Soc.* **1990**, *112*, 173–178. Budnikova, Yu. G.; Yakhvarov, D. G.; Morozov, V. I.; Kargin, Yu. M.; Il'yasov, A. V.; Vyakhireva, Yu. N.; Sinyashin, O. G. *Russ. J. Gen. Chem.* **2002**, *72*, 168–172.

(22) Greatti, A.; Scarpellini, M.; Peralta, R. A.; Casellato, A.; Bortoluzzi, A. J.; Xavier, F. R.; Jovito, R.; Aires de Brito, M.; Szpoganicz, B.; Tomkowicz, Z.; Rams, M.; Haase, W.; Neves, A. *Inorg. Chem.* **2008**, *47*, 1107–1119.

(23) (a) Holman, T. R.; Hendrich, M. P.; Que, L., Jr. *Inorg. Chem.* **1992**, *31*, 937–939. (b) Gultneh, Y.; Khan, A. R.; Ahvazi, B.; Butcher, R. J. *Polyhedron* **1998**, *17*, 3351–3360.